

Classification of Suspected Liver Metastases Using fMRI Images: A Machine Learning Approach

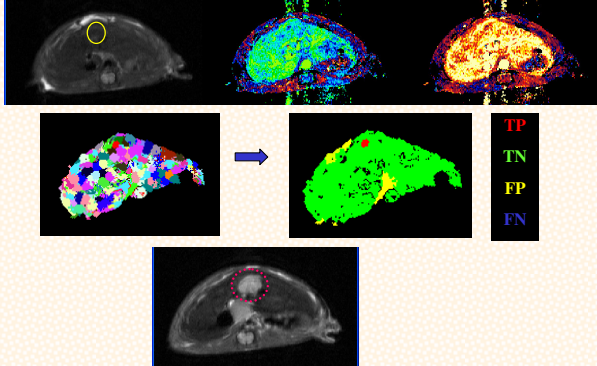
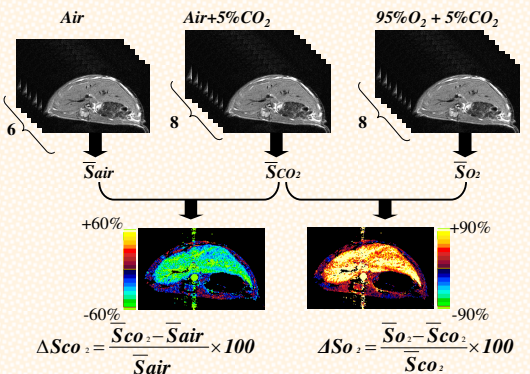
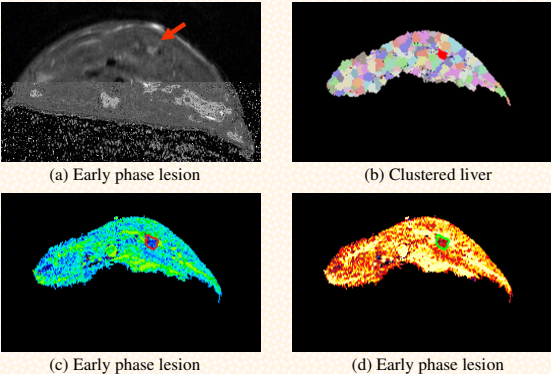
M. Freiman¹, Y. Edrei^{2,3}, Y. Sela¹, Y. Shmidmayer¹, E. Gross⁴, L. Joskowicz¹ and R. Abramovitch^{2,3}

1. School of Engineering and Computer Science, The Hebrew University of Jerusalem, Israel.
2. The G. Savad Institute for Gene Therapy, 3. MRI/MRS Laboratory HBRC, 4. Department of Pediatric Surgery, Hadassah Hebrew University Medical Center, Jerusalem, Israel.

Website: <http://www.cs.huji.ac.il/~caslab/site>

Email: freiman@cs.huji.ac.il



1. Introduction	2. Method	3. Experimental results														
<p>Motivation:</p> <ul style="list-style-type: none"> The liver is the most common site of visceral metastases for colorectal carcinoma patients. Hepatic metastases are a frequent clinical complication. Despite the availability of a variety of treatments, hepatic metastases are difficult to eradicate because of their late discovery. Early and accurate detection of these lesions is recognized as having the potential of improving survival rates and reducing treatment morbidity. Previous works used CT or MR with the intravenous administration of a contrast agent which enforces reduction of the spatial resolution. <p>Approach:</p> <ul style="list-style-type: none"> Use fMRI with hypercapnia and hyperoxia for monitoring changes in liver perfusion and hemodynamics. Automatic classification of the colorectal hepatic metastases based on their early hemodynamical changes using Support Vector Machine (SVM) classification engine. <p>Challenges:</p> <ul style="list-style-type: none"> High inter-subject variability in the spatial locations of the metastases Variations of metastases' functional activation response GRE (Gradient Recalled Echo) signal variations of the different tissues. <p>Advantages:</p> <ul style="list-style-type: none"> No need of a contrast agent administration and reduction of the spatial resolution due to the high temporal resolution. The possibility to detect smaller lesions at an earlier development stage. 	<p>Method outline:</p> <ol style="list-style-type: none"> Hemodynamic activity maps computation Maps normalization Functional adaptive partitioning Features extraction Model construction Early classification <p>2. Maps normalization</p> <ul style="list-style-type: none"> Liver borders are determined from the anatomical MRI images and all the rest is eliminated from the maps To overcome the high variability of the GRE signal from different subjects and in the same subject at different time points Each map is centered around a liver mean intensity of zero, with a standard deviation of 1 Each dataset is filtered with bilateral smoothing to eliminate noise In the advanced phase used for training, the lesions were extracted from the anatomical images 	 <p>Example of a partitioned liver from the early growth phase. The suspected region is encircled by the yellow circle. The images in upper line are the anatomical image and functional maps from the early stage. The images in the middle are the partitioned (left) and classified (right) image colored according to the results. The image in the bottom is the anatomical image from the advanced growth phase. The metastasis region corresponds to the suspected region is encircled with a red circle.</p>														
 <p>Hemodynamic activity maps computation. Maps of mean signal intensity (SI) values for each pixel during the different inhaled gases (ΔS_{air}, ΔS_{CO_2} and ΔS_{O_2}) were calculated from 8 repeats for each gas. The percentage of change of fMRI signal intensity induced by hypercapnia (ΔS_{CO_2}) and hyperoxia (ΔS_{O_2}) was calculated using the below equations. Data is presented in color maps as indicated in color-bar.</p> $\Delta S_{CO_2} = \frac{S_{CO_2} - \bar{S}_{air}}{\bar{S}_{air}} \times 100$ $\Delta S_{O_2} = \frac{S_{O_2} - S_{CO_2}}{S_{CO_2}} \times 100$	 <p>Example of a partitioned liver from the early growth phase. The suspected region is pointed by the red arrow</p>	<p>Training database:</p> <ul style="list-style-type: none"> 25 advanced growth phase (days 14-18) datasets + 4 healthy datasets. Each dataset contains 4-5 slices. <p>Test dataset:</p> <ul style="list-style-type: none"> 16 early growth phase (days 10-14). Each dataset contains 4-5 slices. 44 suspected metastases locations selected by an expert. Each location was evaluated at the metastasis' advanced growth phase using anatomical MRI or histology <p>Results:</p> <p>78% accuracy, 88% precision, and of 77% recall</p>														
<p>1. Hemodynamic activity maps computation</p> <ul style="list-style-type: none"> Two hemodynamic activity maps are derived from the fMRI images. The maps describe the mean relative change of the fMRI signal intensity induced by hypercapnia (ΔS_{CO_2}) and hyperoxia (ΔS_{O_2}). The colorectal hepatic metastases are present in regions with reduced ΔS_{O_2} positive values and reduced ΔS_{CO_2} negative values. 	<p>3. Functional adaptive partitioning</p> <p>A mean-shift clustering procedure is applied to the datasets using both spatial and functional information from both maps to partition the data to separate clusters according to their functional activity.</p> <p>4. Features extraction</p> <ul style="list-style-type: none"> A set of histogram-based features is computed from each map for each cluster as follows: 1) mean; 2) standard deviation; 3) kurtosis; 4) skewness, and 5) interquartile range The histograms were normalized to overcome the different sizes of different regions. <p>5. Model construction</p> <ul style="list-style-type: none"> A classification model for each hemodynamic activity map was computed separately. Clusters of healthy liver and metastasis' regions from the advanced growth phase (days 15-18) were used. The model was built using a SVM classification model with a generalized radial basis function kernel. Kernel parameters were tuned experimentally 	<table border="1"> <thead> <tr> <th></th> <th>Positive</th> <th>Negative</th> <th></th> </tr> </thead> <tbody> <tr> <td>Yes</td> <td>23</td> <td>3</td> <td rowspan="3"> <ul style="list-style-type: none"> ★ Accuracy = $\frac{TP+TN}{P+N}$ ★ Precision = $\frac{TP}{TP+FP}$ ★ Recall = $\frac{TP}{P}$ </td> </tr> <tr> <td>No</td> <td>7</td> <td>11</td> </tr> <tr> <td>Total</td> <td>30</td> <td>14</td> </tr> </tbody> </table> <p>Summary of experimental results tabulated in a confusion matrix. The columns indicate the true class (Positive/Negative) and the rows indicate the hypothesized class (Yes/No). The measurements derived from the matrix are summarized at the right.</p> <p>Conclusions</p> <ul style="list-style-type: none"> A new method for the interactive classification of suspected liver metastases using fMRI images at their early growth phase based on classification and clustering methods Experimental results on mice yielded an accuracy of 78% with high precision (88%) This suggests that the method can provide a useful aid for early detection of metastases <p>Future work:</p> <ul style="list-style-type: none"> Human experiments Explore a more suitable clustering method Using advanced features 		Positive	Negative		Yes	23	3	<ul style="list-style-type: none"> ★ Accuracy = $\frac{TP+TN}{P+N}$ ★ Precision = $\frac{TP}{TP+FP}$ ★ Recall = $\frac{TP}{P}$ 	No	7	11	Total	30	14
	Positive	Negative														
Yes	23	3	<ul style="list-style-type: none"> ★ Accuracy = $\frac{TP+TN}{P+N}$ ★ Precision = $\frac{TP}{TP+FP}$ ★ Recall = $\frac{TP}{P}$ 													
No	7	11														
Total	30	14														